

## Optical properties of Ag and Au nanoparticles dispersed within the pores of monolithic mesoporous silica

Weiping Cai<sup>1,3</sup>, H. Hofmeister<sup>1,\*</sup>, T. Rainer<sup>2</sup> and Wei Chen<sup>3</sup>

<sup>1</sup>Max Planck Institute of Microstructure Physics, Weinberg 2, D-06120 Halle, Germany; <sup>2</sup>Department of Physics, Martin-Luther University of Halle-Wittenberg, Friedemann-Bach-Platz 6, D-06108 Halle, Germany;

<sup>3</sup>Institute of Solid State Physics, Chinese Academy of Sciences, Hefei, Anhui 230031, P.R. China;

\*Author for correspondence (Tel.: +49-345-5582677; Fax: +49-345-5511223; E-mail: hof@mpi-halle.mpg.de)

Received 11 May 2001; accepted in revised form 27 June 2001

**Key words:** metal nanoparticles, mesoporous silica, optical absorption, interface interaction, dispersions

### Abstract

The optical absorption of silver and gold nanoparticles dispersed within the pores of monolithic mesoporous silica upon annealing at elevated temperatures has been investigated. With decreasing particle size, the surface plasmon resonance position of the particles blue-shifts first and then red-shifts for silver/silica samples, but only red-shifts for gold/silica samples. This size evolution of the resonance position is completely different from that previously reported for fully embedded particles. We assume a local porosity at the particle/matrix interface, such that free surface of particles within the pores may be in contact with ambient air, and present a two-layer core/shell model to calculate the optical properties. These calculations also consider deviations from the optical constants of bulk matter to account for corresponding effects below about 10 nm particle size. From the good agreement between experimental results and model calculations, we conclude a peculiar particle/ambience interaction dominating the size evolution of the resonance. Because of the difference of core electron structure, the relative importance of the effects of local porosity and free surface, respectively, are different for silver and gold. For silver, the effect of the local porosity is stronger, but for gold the opposite is found.

### Introduction

Nanoparticles often exhibit novel properties, different from those of bulk materials, which strongly depend on size, shape and surface configuration (e.g., Hadjipanayis & Siegel, 1994). Research in this area is mainly motivated by the possibility of designing nanostructured materials that possess novel electronic, optical, magnetic, photochemical and catalytic properties. Extensive studies have been performed for Au and Ag nanosized particles (Hughes & Jain, 1979; Halperin, 1986; Kreibig & Vollmer, 1995; Kreibig et al., 1998) because of their attractive optical properties. They do not only give rise to colour changes, but also to optical enhancements in absorption, Raman scattering, and non-linear effects. According to Mie (Mie, 1908), the

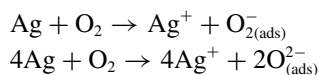
spectral position of the corresponding absorption peak is that frequency  $\omega_r$ , where the sum of the dielectric function of the metal  $\varepsilon(\omega_r)$  and two times the dielectric constant of the surrounding medium  $\varepsilon_m$  equals to zero:  $\varepsilon(\omega_r) + 2\varepsilon_m = 0$ . Usually, the frequency-dependent dielectric function of the particles is approximated by the value of the bulk metal (quasi-static approximation). However, when going below 10 nm particle size, shifts and broadening of the surface plasmon resonance occur because of deviations from the bulk optical constants. The size evolution of the Mie resonance frequency may be understood in terms of classical limitations of the mean free path of electrons due to the particle surface, or due to quantum effects arising from the discreteness in the electron density of states. In both cases, deviations from the bulk

optical constants are concluded. This behaviour has been investigated for free and embedded Ag particles of about 2–10 nm size elsewhere (Cai et al., 2001).

From the viewpoint of basic and of applied research, much attention has been paid to studying the optical properties of nanosized particles dispersed in solution and embedded in glass or polymer matrices (e.g., Edelstein & Cammarata, 1996). However, studies on metal particles dispersed within the pores of monolithic mesoporous solids, being undoubtedly of comparable practical use, are rarely reported in the literature (Yasuda et al., 1987; Cai & Zhang, 1997). Nanoparticles dispersed within the pores of a mesoporous solid are not only in contact with the pore walls, but also exhibit a certain amount of free surface being in contact with ambient air since the pores are interconnected and open. This structural peculiarity will lead to many new physical and chemical effects (Yasuda et al., 1987; Cai et al., 1996; Zhou et al., 1999) due to the chemically active surface of metal particles that do not occur with fully embedded nanoparticle composites. It can be expected that optical properties different from those of non-porous systems will be observed. In this paper, we focus on the optical absorption of Au and Ag nanoparticles dispersed within the pores of monolithic mesoporous silica upon annealing at elevated temperatures.

### Two-layer core/shell model

In contrast to particles fully embedded in a matrix, particles dispersed within the pores of a porous solid exhibit an interface towards the pore walls and also free surface being in contact with ambient air, that is, there is some local porosity at this interface. Taking into account that silica is weakly interacting with the metals silver and gold, it is reasonable to assume no interface reaction, that is, no charge transfer between matrix and particles (Kreibig & Vollmer, 1995). However, surface effects may lead to changes of optical properties of the particles. Ag and Au nanoparticles within the pores are chemically highly surface active due to their small size. Upon exposure to the ambient air, interaction between the particle surface and ambient gas molecules will occur, that is, adsorption or chemisorption on the particle surface. When Ag is in contact with oxygen in air at room temperature, the two following reactions are possible (Kilty & Sachtler, 1974):



that is, chemisorption of  $\text{O}_2$  will occur on Ag particles, as confirmed by differential scanning calorimetry (Cai et al., 1998a). Although gold is inert towards most molecules (e.g., oxygen does not adsorb on clean Au(110) and (111) surfaces (Pireaux et al., 1984), gold clusters smaller than 10 nm in diameter are reactive at room temperature towards  $\text{H}_2$ ,  $\text{CH}_2$ , CO and  $\text{O}_2$  (Cox et al., 1991). Oxygen as well as CO can chemisorb even at  $0^\circ\text{C}$  (Haruta, 1997; Iizuka et al., 1999). The surface chemisorption leads to charge transfer from the metal particle to the adsorbates. Accordingly, we thus assume the free electron dielectric function as being missing in a layer of thickness  $d$  at the particle free surface.

The local porosity at the particle/matrix interface will obviously modify the optical properties of the system (Lerme et al., 1998a,b) due to a matrix dielectric constant much lower than the bulk value in the vicinity of the particle surface. In order to model the effects of local porosity, we simplify it as a hollow shell of thickness  $d_m$  surrounding the particle, with  $d_m$  being a measure of the porosity. Assuming spherical particles, the above-mentioned situation can quantitatively be described by a two-layer core/shell model as schematically shown in Figure 1. Because of transferred or localised free electrons, the dielectric function in the surface layer is different from the particle interior. The dielectric constant in the hollow shell is taken close to the vacuum value. Chemisorbed molecules usually are situated at active sites of the adsorbent surface, but not in a continuous monolayer (Prutton, 1983). Therefore, the dielectric constant of the adsorbate layer can be assumed to be nearly the same as that of air.

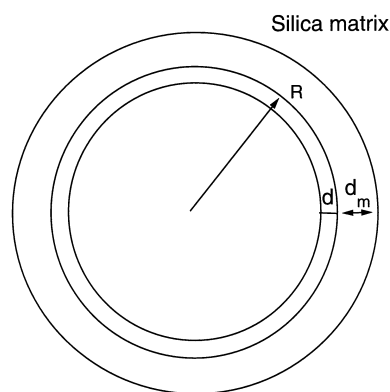


Figure 1. Schematic drawing of the two-layer core/shell model for metal particles within the pores of silica;  $R$ : particle radius,  $d$ : thickness of surface layer,  $d_m$ : thickness of hollow shell.

This is a typical multi-shell problem. Aden and Kerker (1951) and Güttler (1952) extended the Mie theory (Mie, 1908) to spheres with a shell of different material. Bhandari (1985) generalised the matrix formalism of Aden and Kerker to spheres with an arbitrary number of shells in the context of optical detection of air pollution. Recently, Sinzig et al. (1993), Sinzig and Quinten (1994), and Kreibig and Vollmer (1995) have developed a recurrence solution for the general  $h$ -shell problem ( $h = 1, 2, 3, \dots$ ). The corresponding coefficients can be determined by the following formulae:

$$T_n^l = - \frac{\{m_l \psi_n(m_l y_l) [\psi_n'(y_l) + T_n^{l-1} \chi_n'(y_l)] - \psi_n'(m_l y_l) [\psi_n(y_l) + T_n^{l-1} \chi_n(y_l)]\}}{\{m_l \chi_n(m_l y_l) [\psi_n'(y_l) + T_n^{l-1} \chi_n'(y_l)] - \chi_n'(m_l y_l) [\psi_n(y_l) + T_n^{l-1} \chi_n(y_l)]\}}, \quad (1)$$

$$S_n^l = - \frac{\{\psi_n(m_l y_l) [\psi_n'(y_l) + S_n^{l-1} \chi_n'(y_l)] - m_l \psi_n'(m_l y_l) [\psi_n(y_l) + S_n^{l-1} \chi_n(y_l)]\}}{\{\chi_n(m_l y_l) [\psi_n'(y_l) + S_n^{l-1} \chi_n'(y_l)] - m_l \chi_n'(m_l y_l) [\psi_n(y_l) + S_n^{l-1} \chi_n(y_l)]\}}, \quad (2)$$

$$a_n = - \frac{\{m_h \psi_n(m_h y_h) [\psi_n'(y_h) + T_n^{h-1} \chi_n'(y_h)] - \psi_n'(m_h y_h) [\psi_n(y_h) + T_n^{h-1} \chi_n(y_h)]\}}{\{m_h \xi_n(m_h y_h) [\psi_n'(y_h) + T_n^{h-1} \chi_n'(y_h)] - \xi_n'(m_h y_h) [\psi_n(y_h) + T_n^{h-1} \chi_n(y_h)]\}}, \quad (3)$$

$$b_n = - \frac{\{\psi_n(m_h y_h) [\psi_n'(y_h) + S_n^{h-1} \chi_n'(y_h)] - m_h \psi_n'(m_h y_h) [\psi_n(y_h) + S_n^{h-1} \chi_n(y_h)]\}}{\{\xi_n(m_h y_h) [\psi_n'(y_h) + S_n^{h-1} \chi_n'(y_h)] - m_h \xi_n'(m_h y_h) [\psi_n(y_h) + S_n^{h-1} \chi_n(y_h)]\}}, \quad (4)$$

where  $\psi_n(z) = z j_n(z)$ ,  $\chi_n(z) = z y_n(z)$  and  $\xi_n(z) = z h_n^{(1)}(z)$  are the Riccati–Bessel functions.  $n$  is the order of the spherical Bessel functions. The prime denotes the derivation of the function with respect to its argument.  $l = 1, \dots, h$  is the shell number.  $m_l = n_{l+1}/n_l$  represents the relative complex refractive index from the  $(l+1)$ th to the  $l$ th shell. For  $l = h$ , the refractive index  $n_{h+1} = n_m$  corresponds to the refractive index of the host.  $y_l = k_l R_l$ ,  $k_l = 2\pi n_l/\lambda$  is the wave vector in the  $l$ th shell of the medium.  $R_l$  is the radius of the  $l$ th shell.  $T_n^0 = S_n^0 = 0$ .  $a_n$  and  $b_n$  are the Mie coefficients.

As in the case of a compact sphere, the cross-section  $C_{\text{ext}}$  of the extinction of a multi-layer sphere is subject to the following series expansion:

$$C_{\text{ext}} = - \frac{2\pi}{k_m^2} \sum_{n=1}^{\infty} (2n+1) \text{Re}(a_n + b_n), \quad (5)$$

where Re means the real part.

## Model calculations

The dielectric function of the particle surface layer of thickness  $d$  corresponding to the core electron dielectric function  $\varepsilon_d(\omega)$ , can be determined by subtracting the free-electron contribution, parameterised as a Drude–Sommerfeld formula from dielectric data of the bulk metals (Palik, 1985; 1991), and a Kramers–Kronig analysis (Lerme et al., 1998b). For the dielectric function in the particle interior the bulk metal data are modified by size-dependent electron scattering (see Eq. (8) in Hövel et al., 1993). The value for the hollow shell is assumed to be unity.

According to the recurrence solution and dielectric functions of the various regions mentioned above, let the dielectric constant of matrix silica be 2.25, we obtain the Mie scattering coefficients and the corresponding optical extinction spectra for varying particle size, local porosity and surface layer thickness of both particulate composites. The width of the Mie resonance is associated with many factors, such as interface, particle size and its distribution. This has been extensively and thoroughly investigated (Charlé et al., 1984; Hövel et al., 1993; Persson, 1993; Kreibig & Vollmer, 1995; Kreibig et al., 1998; Hilger et al., 2000) and will not be discussed in this paper. Here, we only focus on the evolution of the resonance frequency position.

## Effect of the local porosity without surface layer ( $d = 0$ )

Figure 2 shows the effect of the local porosity of the interface on the surface plasmon resonance position for silver and gold particles of varying radius (1, 3 and 5 nm) in silica under the condition of  $d = 0$ , that is without surface layer. The occurrence of local porosity results in a blue-shift of the resonance. The effect becomes more significant with decreasing particle size. For very large local porosity ( $d_m \rightarrow \infty$ ), the situation of free particles is approached. The resonance position blue-shift with increasing porosity is much stronger for Ag (about 0.4 eV) than for Au (about 0.15 eV). For Au, the effect is obvious only when  $d_m$  is small, but for Ag it occurs in a large range of porosity. That means, the resonance position of Au is nearly insensitive to the dielectric constant of the surrounding medium as compared to the behaviour of Ag.

According to the Mie theory (Mie, 1908), the Mie frequency or resonance frequency  $\omega_r$  is given by solving the approximate equation  $\varepsilon(\omega_r) + 2\varepsilon_m = 0$ , yielding

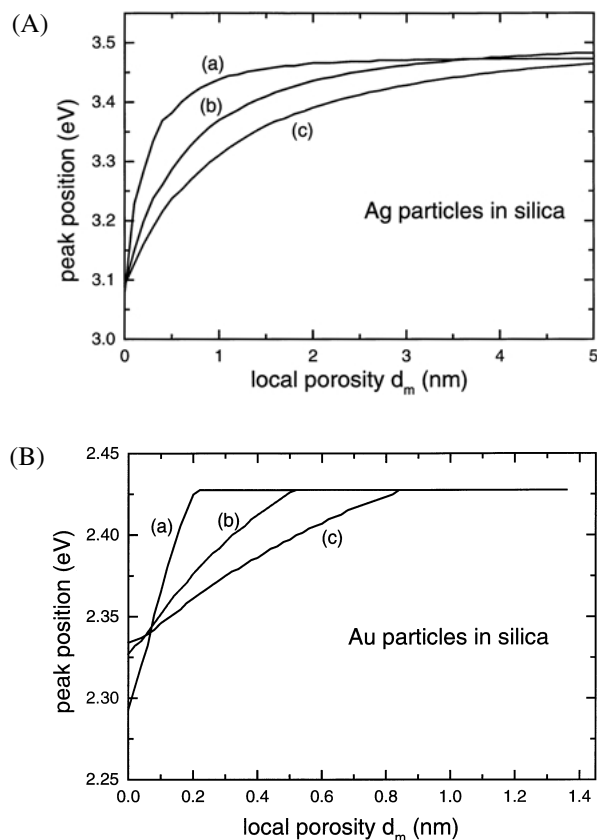


Figure 2. (A) Resonance position versus local porosity for Ag particles in silica without surface layer ( $d = 0$ ); curves (a), (b) and (c): particle radius 1, 3 and 5 nm. (B) Same as (A) for Au particles.

the result:

$$\omega_r = \frac{\omega_p}{\sqrt{2\varepsilon_m + \text{Re}[\varepsilon_d(\omega_r)]}}, \quad (6)$$

where  $\varepsilon_m$  is the dielectric constant of the medium surrounding the particle,  $\varepsilon$  the complex dielectric function of metal particles, and  $\omega_p$  the free electron plasma frequency of the bulk metal which has almost the same value (about 9.1 eV) for both, Ag and Au. Figure 3 shows the real components of  $\varepsilon_d(\omega)$  for the metals Ag and Au (see also Figure 3 in Liebsch, 1993, and Figure 1 in Lerme et al., 1998b, respectively). In the vicinity of the resonance frequency (see the short vertical lines, denoting the Mie frequency for large particles fully embedded in silica), the  $\text{Re}\varepsilon_d$  value of Au is not only about two times as high as that of Ag, but also the slope of the  $\text{Re}\varepsilon_d$  spectrum of Au is much higher than that of Ag (nearly frequency independent below  $\approx 3.0$  eV).

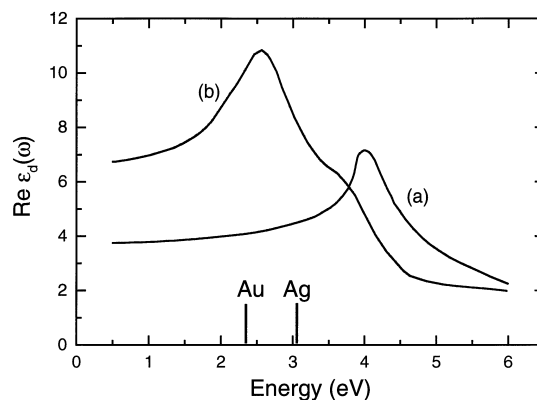


Figure 3. Real component of the complex dielectric function corresponding to the core electrons of (a) silver and (b) gold; short vertical lines denote the resonance position for large particles fully embedded in silica.

This behaviour causes the Au resonance position to be insensitive on dielectric constant changes of the surrounding medium (see Eq. (6)).

#### Effect of the surface layer without local porosity ( $d_m = 0$ )

The effect of the particle surface layer without free electron contribution to the dielectric function on the resonance position, under the condition of no local porosity ( $d_m = 0$ ), is shown in Figure 4(A) and (B) for Au and Ag particles of varying radius (1, 3 and 5 nm) in silica. The resonance position red-shifts nearly linearly with increasing layer thickness  $d$ , and this effect increases with decreasing particle size. Accordingly, the slope of the curves amount to 0.66, 0.22 and 0.14 for Ag particles, and 1.12, 0.44 and 0.29 for Au particles of 1, 3 and 5 nm radius, respectively. In contrast to the effect of local porosity, the resonance frequency of Au is more sensitive to the surface layer than that of Ag. The thickness evolution of the resonance frequency is about 1.5 times steeper for Au than for Ag. This can be attributed to the large difference of the corresponding  $\text{Re}\varepsilon_d$  values in the respective resonance frequency range.

#### Relative importance of both shell effects

To estimate the relative importance of the effects of surface layer and local porosity for the resonance frequency of Ag and Au particles of varying size, we

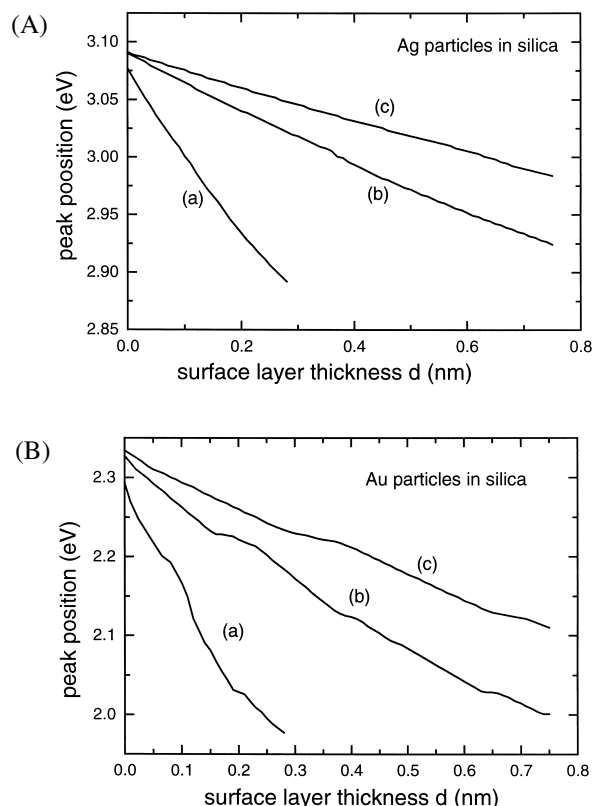


Figure 4. (A) Resonance position versus surface layer thickness for Ag particles in silica without local porosity ( $d_m = 0$ ); curves (a), (b) and (c): particle radius 1, 3 and 5 nm. (B) Same as (A) for Au particles.

superimposed Figures 2 and 4 and plotted the peak shift, related to the fully embedded case ( $d_m = d = 0$ ), versus shell thickness (keeping  $d = d_m$ ) in Figure 5(A) and (B). It is evident that in the initial range of local porosity and surface layer thickness, and in the given range of particle size, the relative importance of both effects is different for Ag and Au. For Ag, the effect of the local porosity on the resonance position shift is larger than that of the surface layer, and increases with reduction of particle size. For Au, however, the reverse situation holds, that is, the effect of the surface layer dominates. Consequently, Ag and Au particles dispersed within the pores of silica should exhibit different behaviour of the resonance position with particle size.

### Experimental procedures

The monolithic mesoporous silica host (planar-like, about 1 mm in thickness) was prepared by sol-gel

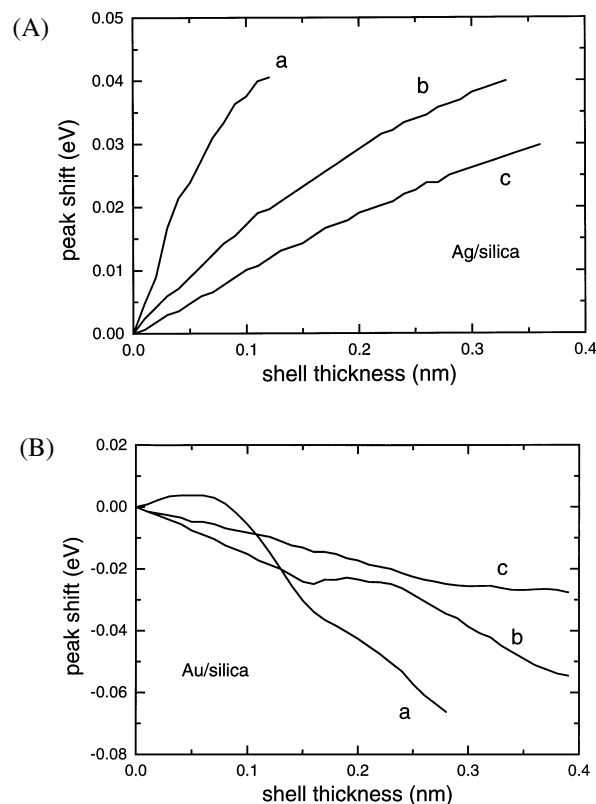


Figure 5. (A) Resonance frequency peak shift for Ag particles in silica considering local porosity and surface layer chemisorption by superimposing Figures 2(A) and 4(A); curves (a), (b) and (c): particle radius 1, 3 and 5 nm. (B) Same as (A) for Au particles.

technique, drying and finally annealing at 800°C for 1 h, as previously described (Cai & Zhang, 1997). The pre-formed host has a specific surface area of about 500 m<sup>2</sup>/g, porosity of about 50% with most of the pores (95% of total pore volume) smaller than 10 nm in diameter, just like a typical mesoporous solid (Hudson & Sequeira, 1993). Au and Ag nanoparticles were *in situ* synthesised within the pores by soaking the host into HAuCl<sub>4</sub> (0.03 M) and AgNO<sub>3</sub> (0.25 M) solutions, respectively, and subsequent heat treatment. For Ag/silica, the soaked samples were dried and initially annealed at 500°C in air for 40 min so as to form Ag particles within the pores as described elsewhere (Cai & Zhang, 1997). Then, pieces of this sample were additionally annealed at 500°C for 20 min, and 500°C, 600°C, 700°C and 800°C for 1 h, respectively. For Au/silica, the samples were dried after soaking and then annealed at 300°C, 500°C and 700°C, respectively, for 1 h in hydrogen atmosphere (AuCl<sub>4</sub><sup>-</sup> can be reduced

by H<sub>2</sub> gas at temperatures above 250°C, see Hosoya et al., 1997) and cooled in air.

Alternatively, to compare possible effects of different routes of synthesis and metal loading, ultrasonic irradiation was utilised for the preparation of Au/silica. First, the silica hosts were impregnated in a mixture of H<sub>2</sub>AuCl<sub>4</sub> solution (1 mM) and the organic additive methanol (0.1 M). The additive was added to capture H• and •OH radicals induced by intense local heating and high pressures owing to ultrasonic irradiation (Meisel, 1979; Westerhausen et al., 1981). The sample soaked into the mixed solution (about 500 ml) was transferred to a conical flask with cover and put in a sonication bath. Before irradiation with 40 kHz ultrasonic wave of 100 W output power at room temperature the flask was purged with argon gas to eliminate oxygen. During irradiation, a water flow for cooling the glass flask in the bath was applied (Oshima et al., 1999). The sample was irradiated for 120 min, sufficient to reduce Au<sup>+</sup> in the pores (Okitsu et al., 1996; Nagata et al., 1996), and then dried at up to 120°C followed by annealing at various temperatures up to 700°C.

The finished samples were investigated by electron microscopy for structural characterisation. To this purpose, the metal loaded samples were ground into powder and dispersed appropriately on carbon supporting films. Optical absorption measurements were conducted at room temperature in the wavelength range from 250 to 800 nm immediately after annealing.

## Results

From the porosity of the host and the ion concentrations of the precursor solutions (Cai & Zhang, 1997), the Ag and Au loading was estimated to be about 1 and 0.25 wt.%, respectively, and  $8 \times 10^{-5}$  for Au in silica by sonication. Electron microscopy examination revealed for all samples uniformly dispersed metal particles of approximately spherical shape. Upon 40 min initial annealing at 500°C of the Ag/silica sample a mean particle size of 2.2 nm is found, that increases to 3.5 and 5 nm upon 20 min and 1 h further annealing at 500°C, respectively. One hour further annealing at 600°C, 700°C and 800°C yields 6, 7.5 and 11.5 nm mean particle size, respectively. For the Au/silica sample, mean particle sizes of 2.9, 8.4 and 11 nm were obtained upon annealing at 300°C, 500°C and 700°C, respectively. Figure 6(A) represents a typical micrograph for Ag/silica (40 + 20 min at 500°C). The corresponding size distribution is given in Figure 6(B). The

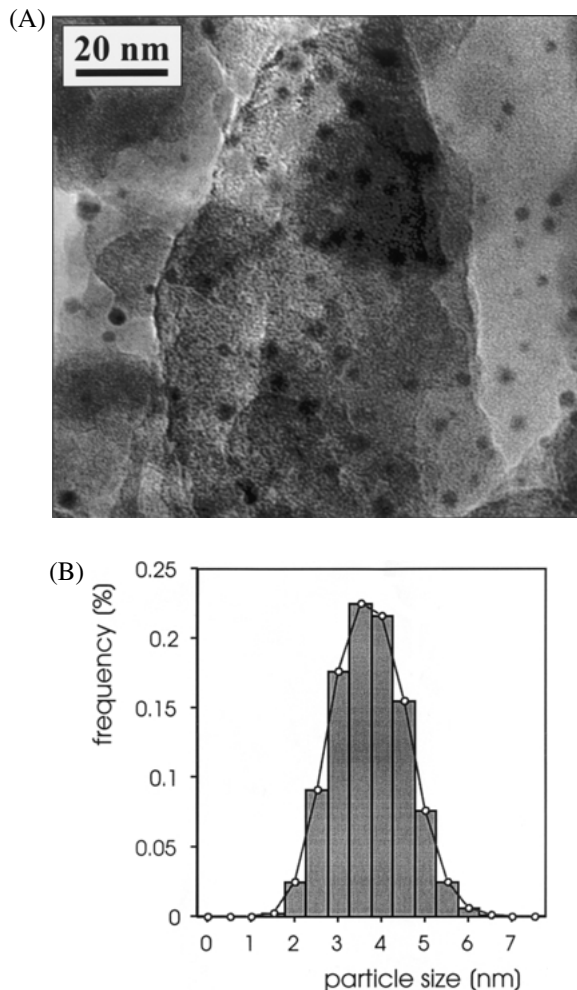


Figure 6. (A) Micrograph of Ag/silica upon annealing at 500°C for 1 h and (B) size distribution of Ag particles in silica as shown in (A).

mean particle size amounts to  $3.5 \pm 0.6$  nm. No aggregation was observed because of the low metal loading, especially for Au/silica samples. The sonicated Au/silica samples have rather low metal loading and only a few Au particles are found by high resolution electron microscopy. So, it is difficult to estimate mean size and size distribution of sufficient statistical accuracy. Nevertheless, the electron microscopy examination still qualitatively indicates an increase of particle size with annealing temperature.

Figures 7 and 8 show the optical absorption spectra for Ag and Au nanoparticles dispersed within the pores of monolithic mesoporous silica annealed at different temperatures. The width of the surface plasmon

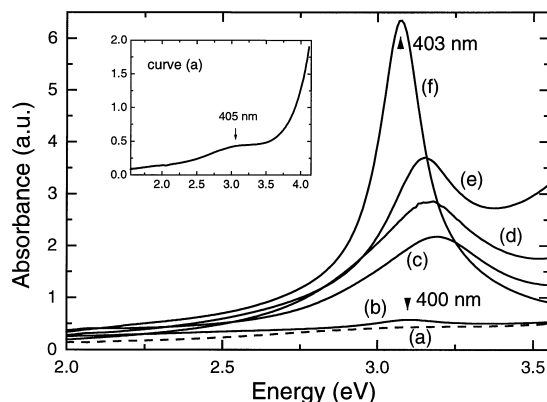


Figure 7. Optical spectra of Ag particles in silica; curve (a): annealing in air 40 min at 500°C, curve (b): additional 20 min at 500°C, curves (c)–(f): additional 1 h at 500°C, 600°C, 700°C and 800°C, respectively.

resonance for both metals increases with decreasing particle size or annealing temperature, respectively. This is in agreement with previously reported findings on embedded particle systems. As may be recognised from Figure 7, for Ag/silica the peak positions, however, blue-shifts first and then red-shifts. This deviates from the previously reported behaviour of, e.g., Ag particles in vacuum, argon and alumina which show blue-shift (Borensztein et al., 1986; Charlé et al., 1989; Hövel et al., 1993; Lerme et al., 1998b), and in glass, which show quasi-size independence (Kreibig et al., 1998) or red-shift (Smithard, 1973). For Au/silica samples of both routes of synthesis, H<sub>2</sub> reduction and ultrasonic irradiation, the resonance position exhibits the same evolution trend with annealing temperature as shown in Figure 8(A) and (B). That means, it only red-shifts with decreasing particle size, in contrast to Au particles in glass (Kreibig, 1977) which exhibit a slight blue-shift, and in alumina where an obvious blue-shift occurs (Palpant et al., 1998). In other words, the shift trends for both metals are different from each other and from the corresponding cases of fully embedded particles.

## Discussion

As mentioned above, in the nanoparticulate composites studied, that is, metal nanoparticles dispersed within the pores of monolithic mesoporous silica, the particle/matrix interface is modified by a local porosity and free particle surface being in contact with ambient

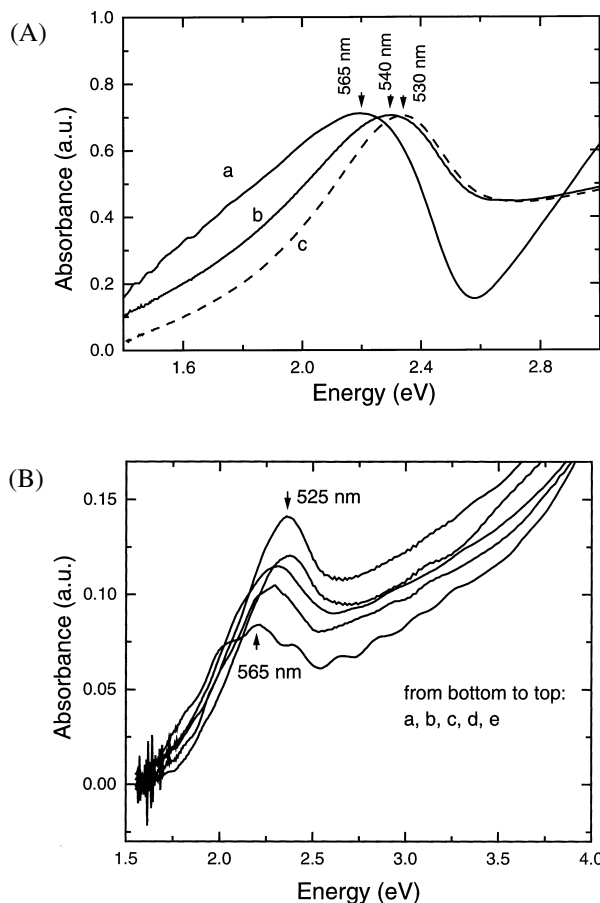


Figure 8. (A) Optical spectra of Au particles in silica; curves (a)–(c) annealing 1 h in hydrogen at 300°C, 500°C and 700°C, respectively. (B) Optical spectra of Au particles in silica (ultrasonic irradiation); curve (a): upon drying at 120°C, curve (b): plus annealing 1 h at 500°C, curve (c): additional 10 min at 600°C, curve (d): additional 10 min at 700°C, curve (e): additional 65 min at 700°C.

air. It is evident that any interface reaction may influence the optical absorption and result in a red-shift of the resonance with decreasing particle size (Hosoya et al., 1997) due to the reduction of free electron density induced by charge transfer. Up to now, however, such results were not reported for Au and Ag particles fully embedded in silica. Instead of a red-shift, mostly a blue-shift, or quasi-size independence of the resonance position with decreasing particle size (Hövel et al., 1993; Kreibig, 1997; Kreibig et al., 1998) was found. Since silica is a weakly interacting matrix, any interface reaction with Ag or Au may be neglected. The size evolution of the resonance position in our samples

mainly does not originate from interactions across the interface. In addition, in our samples, the area of contact along the interface to the pore walls is much less than for fully embedded particles. Aggregates of particles such as touching spheres, that may also cause a red-shift of the resonance (Clippe et al., 1976; Kreibig & Genzel, 1985), were excluded by electron microscopy investigation because of the low particle loading, especially for the sonicated samples. Despite the resonance band broadening effect of a particle size distribution, the resonance position is found remarkably insensitive to the occurrence of size distributions with log-normal, Gaussian or triangular shape function (Granqvist & Hunderi, 1977), respectively. Therefore, the effect of the size distribution was mostly neglected in the literature on the particle size evolution of the Mie resonance (Granqvist & Hunderi, 1977; Lerme et al., 1998a,b; Palpant et al., 1998). Concerning the size evolution of the resonance position, we suggest it is mainly resulting from a combination of both, the local porosity leading to a blue-shift, and the localised electron surface layer inducing a red-shift, respectively. Due to the difference of the respective core electron structure, the relative importance of both effects is different for Ag and Au which is reflected by the corresponding Mie resonance evolution with particle size.

To consider the chemisorption of species from the ambient, we assume that free electrons are transferred or localised only in the surface monolayer, independent on the particle size. Accordingly, we can calculate the optical extinction for Ag and Au using the bulk interatomic distance (0.25 nm). Figure 9(A) and (B) represents the optical extinction spectra calculated according to the two-layer model for Ag and Au particles of varying size assuming  $d = d_m = 0.25$  nm. By the comparison with Figures 7 and 8, it is evident that the theoretical results are in qualitative agreement with the experiments as for the size evolution trend of the resonance position. Quantitatively, however, there is some difference between the calculated and measured data. Actually, there should be a certain change in local porosity due to particle growth processes during annealing. As reported elsewhere (Cai et al., 1998b), some larger particles are found to grow upon annealing, while the others became smaller, comparable to Ostwald ripening (Verhoeven, 1975) where larger particles grow at the expense of smaller ones. Consequently, considering no porosity change of the silica host below 800°C (Cai et al., 1998), the local porosity will decrease for growing particles upon annealing, but for the others it will increase.

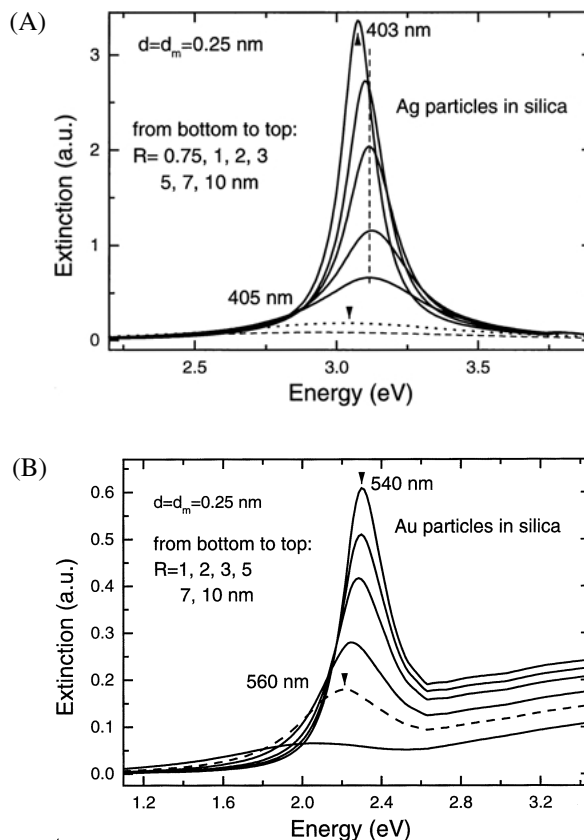


Figure 9. (A) Extinction spectra for Ag particles in silica of varying radius calculated under consideration of local porosity and chemisorption surface layer of monolayer thickness ( $d = d_m = 0.25$  nm). (B) Same as (A) for Au particles.

Figure 10(A) and (B) shows the size evolution of the resonance position for Ag/silica and Au/silica, respectively, calculated for varying contributions from local porosity and surface layer. For comparison, the experimental data are also included. The calculations indicate that neglecting the surface effect (i.e.,  $d = 0$ ) gives rise to a blue-shift of the resonance with decreasing particle size due to the local porosity, as shown by curves (c) in Figure 10. The fully embedded case (i.e.,  $d = d_m = 0$ ) exhibits a quasi-size independent evolution, as shown by curves (d), in agreement with the results of Kreibig (Kreibig, 1977; Kreibig et al., 1998). Obviously, these cases do not meet our experimental results. However, consideration of both, surface layer and local porosity, fairly well agrees with the experimental data given in curves (a) and (b) in Figure 10(A) and (B). The experimental data mostly appear in the range of porosity  $d_m$  between 0.25 and 0.5 nm when

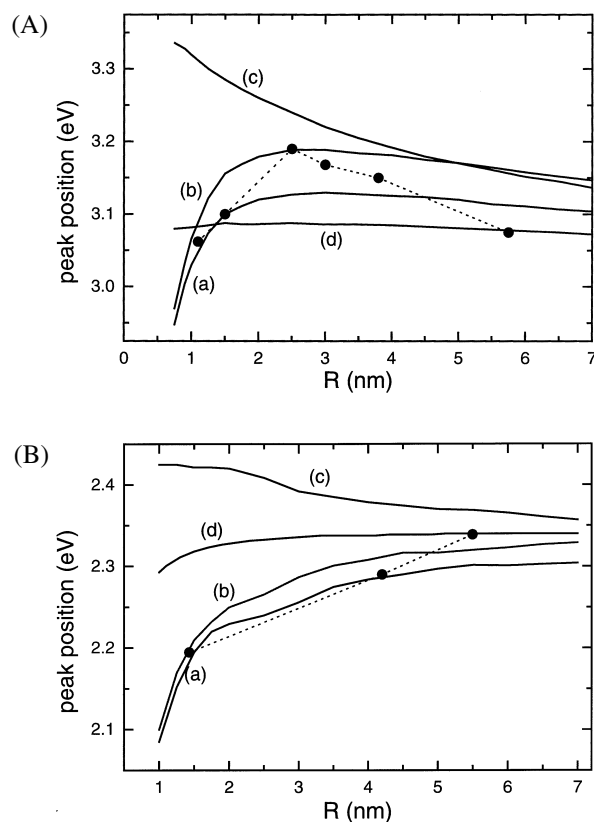


Figure 10. (A) Resonance frequency position versus particle radius for Ag particles in silica considering varying extent of local porosity and surface layer thickness; curve (a):  $d = 0.25$  nm,  $d_m = 0.25$  nm, curve (b):  $d = 0.25$  nm,  $d_m = 0.5$  nm, curve (c):  $d = 0$ ,  $d_m = 0.25$  nm, curve (d):  $d = d_m = 0$ ; solid circles: measured data from Figures 7 and 8 (dot line is to aid the eye). (B) Same as (A) for Au particles.

considering a monolayer without free electrons at the particle surface (i.e.,  $d = 0.25$  nm).

For Ag/silica, the mean particle size increases from 2.2 nm upon initial heat treatment to 3.5 nm upon 20 min additional annealing at 500°C, and to 5 nm for another 1 h at 500°C. Simultaneously, the local porosity increases on an average because of the accompanying size reduction of the small particle portion. Annealing at higher temperatures, however, leads to a decrease of the local porosity since, due to particle growth processes, the interface to the pore walls is growing as well. Upon annealing at 800°C, when growing particles of sizes above 10 nm completely touch the pore walls, the porosity largely may be ignored. Consequently, no chemisorption on the particle surface will occur and the resonance position is that of fully embedded particles.

For Au/silica by H<sub>2</sub> reduction samples, the mean particle diameter upon annealing at 700°C again is larger than 10 nm and the local porosity is assumed nearly to vanish. For such large Au particles also chemisorption on the surface can be neglected (Cox et al., 1991) and the resonance position corresponds to fully embedded particles. Obviously, the theoretical results are in good agreement with the measured data. For the Au/silica by ultrasonic irradiation sample, we have no data for quantitative comparison, but qualitatively the size evolution trend of their resonance is in agreement with curves (a) and (b) of Figure 10(B). It is the effect of the particle surface and the local porosity at the interface that cause size evolution trends of the surface plasmon resonance position different from the corresponding fully embedded systems. Both effects are less well pronounced with increasing particle size.

## Conclusions

The optical properties of Ag and Au nanoparticles dispersed within the pores of monolithic mesoporous silica are governed in a peculiar way by particle/ambience interactions. Depending on the annealing induced variation of particle size, a characteristic shift of the surface plasmon resonance frequency is observed that differs for both metals and from the corresponding cases of fully embedded particles. A two-layer core/shell model is introduced to account for the effects of local porosity at the particle/matrix interface and of free particle surface being in contact with the ambient air. The good agreement of model calculations with the experimental findings confirm that a combination of both effects dominates the observed Mie resonance evolution with particle size. Due to the difference of the respective core electron structure, the relative importance of both effects is different for Ag and Au. With decreasing size, the surface plasmon resonance position of Ag particles in silica blue-shifts first and then red-shifts, but only red-shifts for gold particles in silica.

## References

- Aden A.L. & M. Kerker, 1951. Scattering of electromagnetic waves from two concentric spheres. *J. Appl. Phys.* 22, 1242–1245.
- Bhandari R., 1985. Scattering coefficients for a multilayered sphere: analytic expressions and algorithms. *Appl. Opt.* 24, 1960–1967.

- Borensztein Y., P. De Andres, R. Monreal, J. Lopez-Rios & F. Flores, 1986. Blue shift of the dipolar plasma resonance in small silver particles on an alumina surface. *Phys. Rev. B* 33, 2828–2830.
- Cai W., M. Tan, G. Wang & L. Zhang, 1996. Reversible transition between transparency and opacity for porous silica host dispersed with silver nanometer particles within its pores. *Appl. Phys. Lett.* 69, 2980–2982.
- Cai W. & L. Zhang, 1997. Synthesis and structural and optical properties of mesoporous silica containing silver nanoparticles. *J. Phys.: Condens. Matter* 9, 7257–7267.
- Cai W. & L. Zhang, 1998. Ambience-induced alternating change of optical absorption for the porous silica host loaded with silver nanometer particles. *Appl. Phys. A* 66, 419–422.
- Cai W., Y. Zhang, J. Jia & L. Zhang, 1998a. Semiconducting optical properties of silver/silica mesoporous composite. *Appl. Phys. Lett.* 73, 2709–2711.
- Cai W., L. Zhang, H. Zhong & G. He, 1998b. Annealing of mesoporous silica with silver nanoparticles within in ist pores from isothermal sorption. *J. Mater. Res.* 13, 2888–2895.
- Cai W., H. Hofmeister & M. Dubiel, 2001. Importance of lattice contraction in surface plasmon resonance shift for free and embedded silver particles. *Eur. Phys. J. D* 13, 245–253.
- Charlé K.P., F. Frank & W. Schulze, 1984. The optical properties of silver microcrystallites in dependence on size and the influence of the matrix environment. *Ber. Bunsenges. Phys. Chem.* 88, 350–354.
- Charlé K.P., W. Schulze & B. Winter, 1989. The size dependent shift of the surface plasmon absorption band of small spherical metal particles. *Z. Phys. D* 12, 471–475.
- Clippe P., R. Evrard & A.A. Lucas, 1976. Aggregation effect on the infrared absorption spectrum of small ionic crystals. *Phys. Rev. B* 14, 1715–1721.
- Cox D.M., R. Brickman, K. Creegan & A. Kaldor, 1991. Gold clusters – reactions and deuterium uptake. *Z. Phys. D* 19, 353–355.
- Edelstein A.S. & R.C. Cammarata, 1996. *Nanomaterials: Synthesis, Properties and Applications*. Institute of Physics Publishing, Bristol.
- Granqvist C.G. & O. Hunderi, 1977. Optical properties of ultra-fine gold particles. *Phys. Rev. B* 16, 3513–3534.
- Güttler A., 1952. Die Miesche Theorie der Beugung durch dielektrische Kugeln mit absorbierendem Kern und ihre Bedeutung für Probleme der interstellaren Materie und des atmosphärischen Aerosols. *Ann. Phys.* 11, 65–98.
- Hadjipanayis G.C. & R.W. Siegel, 1994. *Nanophase Materials: Synthesis – Properties – Applications*. Kluwer, Dordrecht.
- Halperin W.P., 1986. Quantum size effects in metal particles. *Rev. Mod. Phys.* 58, 533–606.
- Haruta M., 1997. Size- and support-dependency in the catalysis of gold. *Catalysis Today* 36, 153–166.
- Hilger A., N. Cüppers, M. Tenfelde & U. Kreibig, 2000. Surface and interface effects in the optical properties of silver nanoparticles. *Eur. Phys. J. D* 10, 115–118.
- Hövel H., S. Fritz, A. Hilger, U. Kreibig & M. Vollmer, 1993. Width of cluster plasmon resonances: bulk dielectric functions and chemical interface damping. *Phys. Rev. B* 48, 18178–18188.
- Hosoya Y., T. Suga, T. Yanagawa & Y. Kurokawa, 1997. Linear and nonlinear optical properties of sol-gel-derived Au nanometer-particle-doped alumina. *J. Appl. Phys.* 81, 1475–1480.
- Hudson M. & C.A. Sequeira, 1993. *Multifunctional mesoporous inorganic solids*. Kluwer, Dordrecht.
- Hughes A.E. & S.C. Jain, 1979. Material colloids in ionic crystals. *Adv. Phys.* 28, 717–828.
- Iizuka Y., T. Tode, T. Takao, K. Yatsu, T. Takeuchi, S. Tsubota & M. Haruta, 1999. A kinetic and adsorption study of CO oxidation over unsupported fine gold powder and over gold supported on titanium dioxide. *J. Catalysis* 187, 50–58.
- Kilty P.A. & W.M. Sachtler, 1974. The mechanism of selective oxidation of ethylene to ethylene oxide. *Catal. Rev. Sci. Eng.* 10, 1–16.
- Kreibig U., 1977. Anomalous frequency and temperature dependence of the optical absorption of small gold particles. *J. Physique* 38, C2-97–C2-103.
- Kreibig U. & L. Genzel, 1985. Optical absorption of small metallic particles. *Surf. Sci.* 156, 678–700.
- Kreibig U. & M. Vollmer, 1995. *Optical Properties of Metal Clusters*. Springer Verlag, New York.
- Kreibig U., M. Gartz, A. Hilger & H. Hövel, 1998. Optical investigations of surfaces and interfaces of metal clusters. *Adv. Met. Semicond. Clusters* 4, 345–393.
- Lerme J., B. Palpant, B. Prevel, M. Pellarin, M. Treilleux, J.L. Vialle, A. Perez & M. Broyer, 1998a. Quenching of size effects in free and matrix-embedded silver clusters. *Phys. Rev. Lett.* 80, 5105–5108.
- Lerme J., B. Palpant, B. Prevel, E. Cottancin, M. Pellarin, M. Treilleux, J.L. Vialle, A. Perez & M. Broyer, 1998b. Optical properties of gold metal clusters: A time-dependent local-density-approximation investigation. *Eur. Phys. J. D* 4, 95–108.
- Liebsch A., 1993. Surface-plasmon dispersion and size dependence of Mie resonance: silver versus simple metals. *Phys. Rev. B* 48, 11317–11328.
- Meisel D., 1979. Catalysis of hydrogen production in irradiated aqueous solutions by gold sols. *J. Am. Chem. Soc.* 101, 6133–6135.
- Mie G., 1908. Beiträge zur Optik trüber Medien, speziell kolloidaler Metallösungen. *Ann. Phys.* 25, 377–445.
- Nagata Y., Y. Mizukoshi, K. Okitsu & Y. Maeda, 1996. Sonochemical formation of gold particles in aqueous solution. *Radiat. Res.* 146, 333–338.
- Okitsu K., Y. Mizukoshi, H. Bandow, Y. Maeda, T. Yamamoto & Y. Nagata, 1996. Formation of noble metal particles by ultrasonic irradiation. *Ultrasonics Sonochem.* 3, S249–S251.
- Oshima R., T.A. Yamamoto, Y. Mizukoshi, Y. Nagata & Y. Maeda, 1999. Electron microscopy of noble metal alloy nanoparticles prepared by sonochemical methods. *NanoStruct. Mater.* 12, 111–114.
- Palik E.D., 1985; 1991. *Handbook of Optical Constants of Solids*, Vols I and II. Academic Press, New York.
- Palpant B., B. Prevel, J. Lerme, E. Cottancin, M. Pellarin, M. Treilleux, A. Perez, J.L. Vialle & M. Broyer, 1998. Optical properties of gold clusters in the size range 2–4 nm. *Phys. Rev. B* 57, 1963–1970.
- Persson B.N.J., 1993. Polarizability of small spherical metal particles: influence of the matrix environment. *Surf. Sci.* 281, 153–162.

- Pireaux J.J., M. Chtaib, J.P. Delrue, P.A. Thiry, M. Liehr & R. Caudano, 1984. Electron spectroscopic characterization of oxygen adsorption on gold surfaces. *Surf. Sci.* 141, 211–232.
- Prutton M., 1983. *Surface Physics*, Chapter 6. Oxford Physics Series, Clarendon, Oxford.
- Sinzig J., U. Radtke, M. Quinten & U. Kreibitz, 1993. Binary clusters: homogenous alloys and nucleus-shell structure. *Z. Phys. D* 26, 242–245.
- Sinzig J. & M. Quinten, 1994. Scattering and absorption by spherical multilayer particles. *Appl. Phys. A* 58, 157–162.
- Smithard M.A., 1973. Size effect on the optical and paramagnetic absorption of silver particles in a glass matrix. *Solid State Commun.* 13, 153–156.
- Verhoeven J.D., 1975. *Fundamentals of Physical Metallurgy*. John Wiley, New York.
- Westerhausen J., A. Henglein & J. Lilie, 1981. Radiation-electrochemistry of the colloidal gold microelectrode – hydrogen formation by organic free-radicals. *Ber. Bunsenges. Phys. Chem.* 85, 182–189.
- Yasuda T., H. Komiyama & K. Tanaka, 1987. Gas-sensitive electrical-conduction and its mechanism in a Ag/insulator system with locally discontinuous structure. *Jpn. J. Appl. Phys.* 26, 818–824.
- Zhou H., W. Cai & L. Zhang, 1999. Photoluminescence of indium-oxide nanoparticles dispersed within the pores of mesoporous silica. *Appl. Phys. Lett.* 75, 495–497